Navigation and Control Scheme for Space Rendezvous and Docking With Maneuvering Noncooperative Target Based on Dynamic Compensation

DONGHUI LYU[1], JIONGQI WANG[1], ZHANGMING HE[1,2],
BOWEN HOU[1,2], HAIYIN ZHOU[1], AND DAYI WANG[2]
[1]College of Liberal Arts and Science, National University of Defense Technology, Changsha 410073, China
[2]Beijing Institute of Spacecraft System Engineering, China Academy of Space Technology, Beijing 100094, China

Corresponding author: Jiongqi Wang (wjq_gfkd@163.com)

ABSTRACT Rendezvous and docking with noncooperative targets is one of the key technologies for on-orbit service such as satellite maintenance, space supply and space debris cleaning, etc. For the rendezvous and docking with maneuvering noncooperative targets, a relative measurement scheme based on one monocular camera and one distance sensor is designed. A dynamic compensation filter (DCF) is also proposed to estimate the relative state and the unknow maneuver of the noncooperative target. Meanwhile, the control scheme to fulfill the rendezvous and docking mission is given. Compared with the extended Kalman filter (EKF) and variable state dimension estimator (VSDE), the numerical simulation results demonstrate that the proposed estimator has better performance in estimating the relative state and target maneuver. The control scheme based on DCF can accomplish the rendezvous and docking task when the noncooperative target performs time-varying maneuvers.

INDEX TERMS Noncooperative target, unknown maneuver, space rendezvous and docking, navigation, control.

I. INTRODUCTION

In recent decades, the number of space satellites has increased dramatically. Noncooperative targets such as disabled satellites and space debris threaten the safety of satellites in normal service [1] [2]. On-orbit service including satellite maintenance, space supply and space debris cleaning has become a new concept in the field of space technology. While rendezvous and docking with noncooperative target is one of the key technologies for on-orbit service [3]– [5]. The rendezvous and docking mainly involves the relative measurement and state estimation to the noncooperative target.

The associate editor coordinating the review of this manuscript and approving it for publication was Seung-Hyun Kong.

Due to the limitations of power consumption and quality of satellite, and the lightweight and low-cost characteristics of optical cameras [6] [7], the angles-only relative navigation system based on only an optical camera has developed and been successfully applied to the rendezvous and docking tasks with noncooperative target in recent years. For example, Luo *et al*. [8] proposed an angles-only relative navigation and closed-loop guidance system for spacecraft proximity operations. Zhang *et al*. [9] combined angles-only relative navigation and offline trajectory planning to provide a practical framework for rendezvous operations. However, most of these studies assume that the noncooperative target has no self-maneuver and the state transformation can be accurately modeled. The condition may not be satisfied to the noncooperative targets [10]–[12]. In addition, the angles-only

navigation has a well-known problem of range observability, which needs to be overcomed by the appropriate maneuver of the spacecraft itself [13]–[15]. However, when the target has unknown maneuvering, the observability condition may not be satisfied. Therefore, in order to accomplish the space rendezvous and docking task with maneuvering noncooperative target, a relative measurement scheme based on one monocular camera and one distance sensor is designed. The scheme can not only meet the quality and energy consumption requirements of on-orbit satellites, but also overcome the range observability problem [16].

When the noncooperative targets maneuver, the difficulties of state estimation lie in the inability to establish the accurate dynamic model. The traditional Kalman filter (KF) and extended Kalman filter (EKF) may diverge if the state transition equation is inaccurate [17] [18]. In order to demolish the existing obstacle, some methods have been proposed. The covariance inflation method greatly expands the covariance matrix to increase the weight of current observation [19]–[21]. The filter divergence can be prevented when the target maneuvers. However, the method cannot deal with long-term target maneuvering effectively because it pulls the expanded observation uncertainty into the state estimation. The augmented Kalman filter (AKF) [22] takes the unknown maneuver as a part of the system state and models it as a first-order stationary Markov process driven by white noise. When the target maneuver is constant, AKF performs excellently. But if the maneuver is time-varying, the AKF performance will decline dramatically. Input estimation (IE) [23] [24] algorithm detects and directly estimates the unknown maneuvers. The interacting multiple model (IMM) [25] is widely applied to the state estimation of maneuvering targets [26] [27]. Both IE and IMM can effectively estimate the constant unknown maneuvering, but their performance will drop sharply for the time-varying unknown maneuvering. Guang et.al. proposed a variable structure estimator (VSE) [11] and observation enhanced Kalman filter (OEKF) [28] based on input compensation. These two methods can dynamically estimate constant and time-varying unknown maneuvers when each component of the system state can be observed or can be solved from the observation. However, the condition may not be satisfied in the case of limited observation.

Aiming at the above challenges, i.e. the limitations of observation and difficulties of estimation when the noncooperative target carries out the unknown maneuver(constant or time-varying), this paper has done the following innovative works to complete the navigation and control related to the space rendezvous and docking with maneuvering noncooperative target. Firstly, a noncooperative target relative measurement scheme based on only one monocular camera and one distance sensor is designed. The monocular camera is used to observe the direction of the target's line-of-sight and the distance sensor to measure the relative distance. This scheme not only meets the requirements of observation, but also satisfies the restrictions of satellite on the quality and energy consumption of observation equipment. Besides,

a maneuvering detector is constructed to detect the existence of noncooperative target maneuver. Meanwhile a state filtering algorithm based on dynamic compensation named dynamic compensation filter (DCF) is proposed to realize the effective estimation of relative state and target maneuver. The main improvement of DCF lies in the high accuracy estimation under the condition of limited observation. In particular, it accomplishes the estimation of relative state and target maneuver when the maneuver is time–varying, which has not been not well solved. Moreover, DCF is combined with the multi-pulse maneuver strategy in [29] to establish the control scheme for the space rendezvous and docking mission with maneuvering noncooperative target. Finally, the simulation results verify the effectiveness of the proposed filter and the control scheme.

This paper will be organized in the following order. Section II describes the scenario of space rendezvous and docking with noncooperative target. The relative motion equation and measurement model are also given. DCF based on a target maneuvering detector is constructed in Section III. Section IV derives the control scheme for the space rendezvous and docking mission and Section V carries out the numerical simulations for different maneuvering modes. Finally, Section VI draw the conclusions.

II. SCENARIO DESCRIPTION

Space rendezvous and docking mission refers to the technology making the chasing spacecraft (named chaser) approach and then couple with another target object, which is one of the preconditions and key technologies for on-orbit service.

Suppose the following space rendezvous and docking scenarios: Chaser has arrived at a specific position in space under the guidance of the ground station. The rendezvous and docking task takes place in a circular orbit [30] as shown in Fig. 1, in which the blue curve represents the orbit and the object in front of Chaser is the noncooperative target.

In order to analyze the relative motion between Chaser and the noncooperative target, the coordinate system $\mathcal{T}$ is established firstly and its origin is located at the noncooperative target centroid. x-axis of $\mathcal{T}$ is along the tangent direction of the target orbit, z-axis points to the earth center and y-axis completes the right-handed cartesian coordinate system. The positive direction of x-axis is consistent with the moving direction of the targets.

In the two-body problem, the distance between the chaser and the noncooperative target is much smaller than that between the target and the earth center. So, it can be considered that the chaser and the noncooperative target are in the same circular orbit. The relative motion dynamics can be given by Clohessy-Wiltshire (CW) equation [31] as shown in (1)

$$\begin{bmatrix} \ddot{x} \\ \ddot{y} \\ \ddot{z} \end{bmatrix} = \begin{bmatrix} -2\omega\dot{z} \\ -\omega^2 y \\ 2\omega\dot{x} + 3\omega^2 z \end{bmatrix} + \boldsymbol{u} + \boldsymbol{a} + \boldsymbol{w}. \tag{1}$$
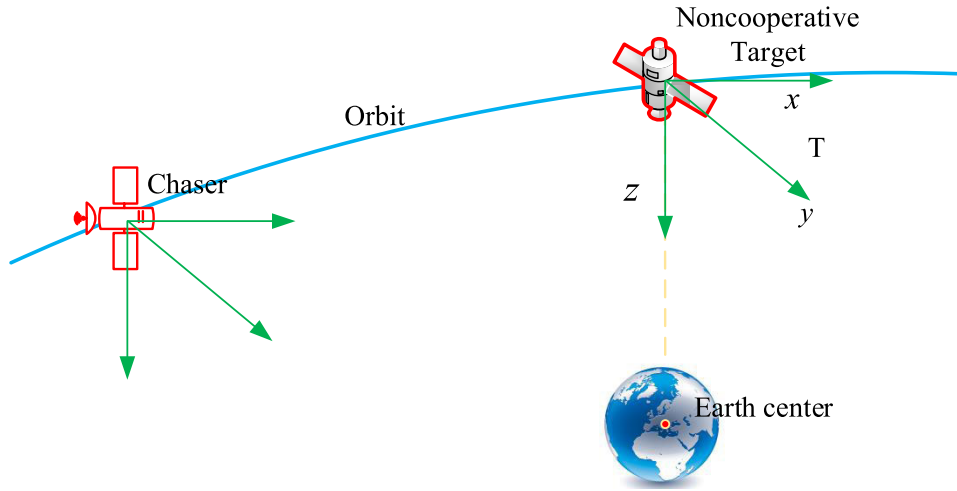
FIGURE 1. Schematic diagram of docking with noncooperative targets.

Where ω denotes the angular velocity of the circular orbit, $x = [x\ y\ z]^T$ is the position vector of chaser relative to noncooperative target in $\mathcal{T}$ coordinate. u and a represent the relative motion acceleration caused by Chaser's own maneuver and the noncooperative target's unknown maneuver respectively. $w \in \mathbb{R}^3$ is the Gaussian white noise with zero mean.

Define the system vector $X = [x^T\ \dot{x}^T]^T$ where $\dot{x} = [\dot{x}\ \dot{y}\ \dot{z}]^T$ is the relative velocity. Without considering the system noise, (1) can be rephrased as

$$\dot{X} = AX + Bu + Ba, \quad (2)$$

where

$$A = \begin{bmatrix} 0 & 0 & 0 & 1 & 0 & 0 \\ 0 & 0 & 0 & 0 & 1 & 0 \\ 0 & 0 & 0 & 0 & 0 & 1 \\ 0 & 0 & 0 & 0 & 0 & -2\omega \\ 0 & -\omega^2 & 0 & 0 & 0 & 0 \\ 0 & 0 & 3\omega^2 & 2\omega & 0 & 0 \end{bmatrix}, B = \begin{bmatrix} 0 & 0 & 0 \\ 0 & 0 & 0 \\ 0 & 0 & 0 \\ 1 & 0 & 0 \\ 0 & 1 & 0 \\ 0 & 0 & 1 \end{bmatrix}. \quad (3)$$

The transition equation of the system as shown in (4) can be derived by discretizing (2).

$$X_{k+1} = \Phi(\tau)X_k + \int_{t_k}^{t_{k+1}} \Phi(t_{k+1} - t)Bu(t)dt$$
$$+ \int_{t_k}^{t_{k+1}} \Phi(t_{k+1} - t)Ba(t)dt, \quad (4)$$

where k and τ denote the time and time step respectively.

$$\Phi(t) = \begin{bmatrix} \Phi_{rr}(t) & \Phi_{rv}(t) \\ \Phi_{vr}(t) & \Phi_{vv}(t) \end{bmatrix}, \quad (5)$$

$$\Phi_{rr}(t) = \begin{bmatrix} 1 & 0 & 6\sin(\omega t) - 6\omega t \\ 0 & \cos(\omega t) & 0 \\ 0 & 0 & 4 - 3\cos(\omega t) \end{bmatrix}, \quad (6)$$

$$\Phi_{rv}(t) = \begin{bmatrix} \frac{-3\omega t + 4\sin(\omega t)}{\omega} & 0 & \frac{2(\cos(\omega t) - 1)}{\omega} \\ 0 & \frac{\sin(\omega t)}{\omega} & 0 \\ \frac{-2\cos(\omega t) + 2}{\omega} & 0 & \frac{\sin(\omega t)}{\omega} \end{bmatrix}, \quad (7)$$

$$\Phi_{vr}(t) = \begin{bmatrix} 0 & 0 & 6\omega(\cos(\omega t) - 1) \\ 0 & -\omega\sin(\omega t) & 0 \\ 0 & 0 & 3\omega\sin(\omega t) \end{bmatrix}, \quad (8)$$

$$\Phi_{vv}(t) = \begin{bmatrix} -3 + 4\cos(\omega t) & 0 & -2\sin(\omega t) \\ 0 & \cos(\omega t) & 0 \\ 2\sin(\omega t) & 0 & \cos(\omega t) \end{bmatrix}. \quad (9)$$

For the specific $u(t)$ and $a(t)$, their integral from t_k to t_{k+1}, $\int_{t_k}^{t_{k+1}} \Phi(t_{k+1} - t)Bu(t)dt$ and $\int_{t_k}^{t_{k+1}} \Phi(t_{k+1} - t)Ba(t)dt$, are equivalent to $G_k u_k$ and $G_k a_k$. Where u_k and a_k are the impulse maneuver of the chaser and the noncooperative target at t_k respectively, and

$$G_k = \begin{bmatrix} \Phi_{rv}(\tau) \\ \Phi_{vv}(\tau) \end{bmatrix}. \quad (10)$$

So (4) can be rephrased as

$$X_{k+1} = \Phi(\tau)X_k + G_k u_k + G_k a_k. \quad (11)$$

Generally, the impulse maneuver of the chaser, i.e. u_k is the system input, and is known. While some measurement information is needed to estimate the relative state X_k and the unknown target maneuver a_k. In order to enhance the system observability for the space rendezvous and docking task, this paper designs a relative measurement scheme based on a monocular camera and a distance sensor to measure the line-of-sight direction and the relative distance.

Assume that the optical center of monocular camera coincides with the mass center of the chaser. The main optical axis is parallel to the x-axis of coordinate $\mathcal{T}$ and the camera lens points to the positive direction of x-axis. According to the standard pinhole camera model [31], the system observation equation can be obtained as follows

$$Z_{k+1} \triangleq h(X_{k+1}) = \begin{bmatrix} \varphi \\ \psi \\ d \end{bmatrix} = \begin{bmatrix} f\frac{y}{x} \\ f\frac{z}{x} \\ \sqrt{x^2 + y^2 + z^2} \end{bmatrix} + v_{k+1}, \quad (12)$$

where f is the focal length of the camera, $[\varphi, \psi]$ is the coordinate of the noncooperative target centroid in the camera imaging plane and d is the relative distance. $\boldsymbol{v}_{k+1} \in \mathbb{R}^3$ is uncorrelated measurement noise. Assume that $\boldsymbol{v}_{k+1}$ obeys the zero mean Gaussian distribution and its covariance matrix is $\boldsymbol{R}_{k+1}$.

$$\boldsymbol{R}_{k+1} = \mathrm{diag}\left(\sigma_\varphi^2, \sigma_\psi^2, \sigma_d^2\right). \tag{13}$$

Remark1: The relative attitude motion is ignored in the docking phases for several reasons. First, the relative attitude motion control is standard and it is not the contribution of this paper. Second, in order to consider attitude motion, CW equation and observation equation can be easily upgraded by introducing coefficient matrices with attitude angles. However, these differences can be fully resolved through simple force or coordinate transformations. So, the simplification indeed does not damage the theoretical contribution of this paper.

Remark2: In addition to CW equations as shown in (1), other relative orbital models such as Tschauner–Hempel (TH) dynamics can also describe the two-body relative motion. Similar to (11), the discrete propagating equation based on TH dynamics can be derived, but with different $\boldsymbol{\Phi}(\tau)$ and $\boldsymbol{G}_k$. However, the differences will not bring fundamental difficulties to the subsequent derivations. After the simple substitution of $\boldsymbol{\Phi}(\tau)$ and $\boldsymbol{G}_k$, DCF and the control framework proposed in this paper can also be applied to the new dynamic models.

Remark3: The challenges faced by this research lie in the following aspects. Firstly, the observation is limited and whether the target has made unknown maneuver needs to be judged. Secondly, it is difficult to estimate the relative state when the state propagating equation has the unknown term, the target maneuver, especially the time-varying one. In the past studies, the state transition model is usually constructed on the assumption that the target maneuver is constant. However, the assumption may be not in line with the reality. Although some studies have studied the estimation of time-varying target maneuvers, the strong observability conditions they require may not be satisfied on the satellite. Therefore, the main improvement of DCF is to estimate the relative state and target maneuver under the condition of limited observation and any possible target maneuver. Thirdly, within the authors' knowledge, the control scheme for rendezvous and docking with maneuvering noncooperative targets has not been proposed.

Remark4: $\int_{t_k}^{t_{k+1}} \boldsymbol{\Phi}(t - t_k) \boldsymbol{B}\boldsymbol{a}(t)dt$, the impact on the relative state resulted from target maneuver, is equivalent to $\boldsymbol{G}_k\boldsymbol{a}_k$ and $\boldsymbol{G}_k$ is known. For the sake of simplicity, the estimation of unknown maneuvers $\boldsymbol{a}(t)$ refers to the estimation of $\boldsymbol{a}_k$ which has the same effect on the relative state as $\boldsymbol{a}(t)$ from t_k to t_{k+1}.

III. STATE ESTIMATION AND DYNAMIC COMPENSATION OF UNKNOWN MANEUVERS
A. EXTENDED KALMAN FILTER
To estimate the relative states and target maneuvers, the extended Kalman filter (EKF) is introduced firstly.

Assume that there is no maneuver of the target from t_k to t_{k+1}, i.e. $\boldsymbol{a}_k = 0$ in (11) and then the state transition equation can be given as follows

$$\boldsymbol{X}_{k+1} \triangleq \boldsymbol{f}(\boldsymbol{X}_k, \boldsymbol{u}_k) = \boldsymbol{\Phi}(\tau)\boldsymbol{X}_k + \boldsymbol{G}_k\boldsymbol{u}_k. \tag{14}$$

If the state estimation at t_k is $\hat{\boldsymbol{X}}_k$ and the corresponding estimation error covariance matrix is $\boldsymbol{P}_k$, EKF gives the state estimation $\hat{\boldsymbol{X}}_{k+1}$ and $\boldsymbol{P}_{k+1}$ through (15) to (20).

$$\hat{\boldsymbol{X}}_{k+1,k} = \boldsymbol{f}\left(\hat{\boldsymbol{X}}_k, \boldsymbol{u}_k\right), \tag{15}$$

$$\boldsymbol{P}_{k+1,k} = \boldsymbol{F}_k\boldsymbol{P}_k\boldsymbol{F}_k^{\mathrm{T}} + \boldsymbol{G}_k\boldsymbol{Q}_k\boldsymbol{G}_k^{\mathrm{T}}, \tag{16}$$

$$\boldsymbol{K}_{k+1} = \boldsymbol{P}_{k+1,k}\boldsymbol{H}_{k+1}^{\mathrm{T}}\left(\boldsymbol{H}_{k+1}\boldsymbol{P}_{k+1,k}\boldsymbol{H}_{k+1}^{\mathrm{T}} + \boldsymbol{R}_{k+1}\right)^{\mathrm{T}}, \tag{17}$$

$$\hat{\boldsymbol{X}}_{k+1} = \hat{\boldsymbol{X}}_{k+1,k} + \boldsymbol{K}_{k+1}\boldsymbol{\eta}_{k+1}, \tag{18}$$

$$\boldsymbol{\eta}_{k+1} = \boldsymbol{Z}_{k+1} - \boldsymbol{h}\left(\hat{\boldsymbol{X}}_{k+1,k}\right), \tag{19}$$

$$\boldsymbol{P}_{k+1} = (\boldsymbol{I}_6 - \boldsymbol{K}_{k+1}\boldsymbol{H}_{k+1})\,\boldsymbol{P}_{k+1,k}(\boldsymbol{I}_6 - \boldsymbol{K}_{k+1}\boldsymbol{H}_{k+1})^{\mathrm{T}} + \boldsymbol{K}_{k+1}\boldsymbol{R}_{k+1}\boldsymbol{K}_{k+1}^{\mathrm{T}}. \tag{20}$$

Where $\boldsymbol{Q}_k \in \mathbb{R}^{3 \times 3}$ is a positive definite system noise covariance matrix. Similar to [32], the $\boldsymbol{Q}_k$ here is actually a performance tuning parameter of EKF. $\hat{\boldsymbol{X}}_{k+1,k}$ is one-step predicted state estimation. $\boldsymbol{P}_{k+1,k}$ is one-step predicted covariance matrix estimation. $\boldsymbol{K}_{k+1}$ denotes the filter gain matrix. $\boldsymbol{\eta}_{k+1}$ is the innovation and $\boldsymbol{I}_6$ is the unit matrix with dimension 6×6.

$$\boldsymbol{F}_k = \left.\frac{\partial \boldsymbol{f}(\boldsymbol{X}, \boldsymbol{u})}{\partial \boldsymbol{X}}\right|_{\boldsymbol{X}=\hat{\boldsymbol{X}}_k} = \boldsymbol{\Phi}(\tau), \tag{21}$$

$$\boldsymbol{H}_{k+1} = \left.\frac{\partial \boldsymbol{h}(\boldsymbol{X})}{\partial \boldsymbol{X}}\right|_{\boldsymbol{X}=\hat{\boldsymbol{X}}_{k+1,k}}$$

$$= \begin{bmatrix} -\dfrac{\hat{\varphi}_{k+1,k}}{\hat{x}_{k+1,k}} & f\dfrac{1}{\hat{x}_{k+1,k}} & 0 & 0\ 0\ 0 \\[2ex] -\dfrac{\hat{\psi}_{k+1,k}}{\hat{x}_{k+1,k}} & 0 & f\dfrac{1}{\hat{x}_{k+1,k}} & 0\ 0\ 0 \\[2ex] \dfrac{\hat{x}_{k+1,k}}{\hat{d}_{k+1,k}} & \dfrac{\hat{y}_{k+1,k}}{\hat{d}_{k+1,k}} & \dfrac{\hat{z}_{k+1,k}}{\hat{d}_{k+1,k}} & 0\ 0\ 0 \end{bmatrix}. \tag{22}$$

where

$$\hat{\varphi}_{k+1,k} = f\frac{\hat{y}_{k+1,k}}{\hat{x}_{k+1,k}},$$

$$\hat{\psi}_{k+1,k} = f\frac{\hat{z}_{k+1,k}}{\hat{x}_{k+1,k}},$$

$$\hat{d}_{k+1,k} = \sqrt{\hat{x}_{k+1,k}^2 + \hat{y}_{k+1,k}^2 + \hat{z}_{k+1,k}^2}. \tag{23}$$

$\left[\hat{x}_{k+1,k}\ \hat{y}_{k+1,k}\ \hat{z}_{k+1,k}\right]^{\mathrm{T}}$ is the one-step relative position prediction, i.e. the first three components of $\hat{\boldsymbol{X}}_{k+1,k}$.

B. TARGET MANEUVER COMPENSATION FLOW AND DESIGN OF MANEUVER DETECTOR
When the noncooperative target has no maneuver, EKF can get the approximately optimal estimation. But when the noncooperative target maneuvers, the conclusion will not hold.
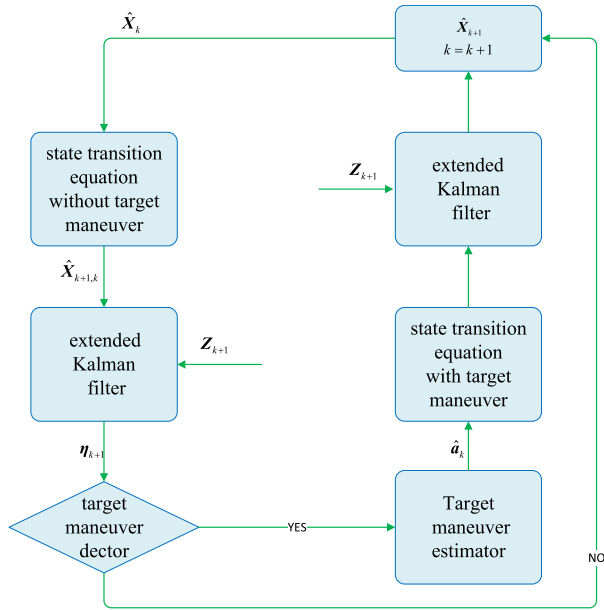
FIGURE 2. Schematic diagram of DCF.

Therefore, DCF for target maneuvering and the relative state estimation is constructed. The structure flow of DCF is shown in Fig. 2

As shown in Fig. 2, DCF takes it for granted that the noncooperative target has no maneuver initially and detects the maneuver through the innovation $\boldsymbol{\eta}_{k+1}$. If the detecting result is positive, the estimation of maneuver, $\hat{\boldsymbol{a}}_k$, will be given by a target maneuver estimator. Next, $\hat{\boldsymbol{a}}_k$ is fed back to the state transition equation and then the modified state estimation is obtained.

The principle of constructing the noncooperative target maneuver detector is as follows. Based on the hypothesis test theory, the statistics, $\theta_{k+1} = \boldsymbol{\eta}_{k+1}^{\mathrm{T}}(\boldsymbol{H}_{k+1}\boldsymbol{P}_{k+1,k}\boldsymbol{H}_{k+1}^{\mathrm{T}} + \boldsymbol{R}_{k+1})\boldsymbol{\eta}_{k+1}$, is established. For the following hypothesis testing problems:

Zero hypothesis γ_0: the noncooperative target has no maneuver

Alternative hypothesis γ_1: the noncooperative target has unknown maneuver

It can be proved that θ_{k+1} approximately obeys the chi–square distribution with the freedom degree of 3, i.e. $\theta_{k+1} \sim \chi^2(3)$. The proof method can be referred to [33].

For the selected confidence level α, it is considered that when $\boldsymbol{\theta}_{k+1} > \chi^2_{\alpha,3}$, the zero hypothesis is rejected and the target is considered to be maneuvering; otherwise, the zero hypothesis is accepted and the target has no maneuvering. $\chi^2_{\alpha,3}$ is the α-quantile of $\chi^2(3)$.

C. TARGET MANEUVER ESTIMATOR
1) CURRENT RELATIVE POSITION ESTIMATION
Next, the derivation process of the relative position estimator from current observations as well as the corresponding estimation accuracy are given.

The observation without considering the observation noise at time $k + 1$ is

$$\boldsymbol{Z}_{k+1} = \begin{bmatrix} \varphi \\ \psi \\ d \end{bmatrix} = \begin{bmatrix} f\dfrac{y}{x} \\ f\dfrac{z}{x} \\ \sqrt{x^2 + y^2 + z^2} \end{bmatrix}. \qquad (24)$$

When the observation noise is not considered, two groups of solutions of the current relative position can be obtained according to the current observation, as shown in (25)

$$\begin{cases} \left[\dfrac{fd}{\sqrt{f^2+\varphi^2+\psi^2}}, \dfrac{d\varphi}{\sqrt{f^2+\varphi^2+\psi^2}}, \dfrac{d\psi}{\sqrt{f^2+\varphi^2+\psi^2}} \right]^{\mathrm{T}} \\ -\left[\dfrac{fd}{\sqrt{f^2+\varphi^2+\psi^2}}, \dfrac{d\varphi}{\sqrt{f^2+\varphi^2+\psi^2}}, \dfrac{d\psi}{\sqrt{f^2+\varphi^2+\psi^2}} \right]^{\mathrm{T}} \end{cases} \qquad (25)$$

This paper assumes that the chaser does not rotate as shown in Fig. 1. To ensure the observability of the system, the first component of the relative position should be always positive or negative in the whole process of rendezvous and docking. Therefore, according to the relative position of the system at the initial time, we can judge which group of solutions is correct. Without losing generality, it is assumed that the correct solution is the first one in (25). That is, the current relative position estimation obtained from observation, $\tilde{\boldsymbol{x}}$, is as follows

$$\begin{aligned} \tilde{\boldsymbol{x}}_{k+1} &\triangleq \boldsymbol{g}(\boldsymbol{Z}_{k+1}) \\ &= \left[\dfrac{fd}{\sqrt{f^2+\varphi^2+\psi^2}}, \dfrac{d\varphi}{\sqrt{f^2+\varphi^2+\psi^2}}, \dfrac{d\psi}{\sqrt{f^2+\varphi^2+\psi^2}} \right]^{\mathrm{T}}. \end{aligned} \qquad (26)$$

Due to the existence of the observation noise, the observation error will be transferred to the relative position estimation, $\tilde{\boldsymbol{x}}$, through the nonlinear function about the observation, $\boldsymbol{g}$. Under the current measurement conditions, it can be considered that the observation noise $\boldsymbol{v}_{k+1}$ is small relative to the observation data. Note that the estimation error caused by the observation noise is $\boldsymbol{\xi}_{k+1} = \begin{bmatrix} \xi_x & \xi_y & \xi_z \end{bmatrix}$, then

$$\boldsymbol{\xi}_{k+1} = J_g(\varphi, \psi, d)\boldsymbol{v}_{k+1} + \mathrm{o}(\boldsymbol{v}_{k+1}). \qquad (27)$$

Where $\mathrm{o}(\boldsymbol{v}_{k+1})$ is the higher-order small quantity of $\boldsymbol{v}_{k+1}$. $J_g(\varphi, \psi, d)$ is the Jacobi matrix of $\boldsymbol{g}$ to $[\varphi, \psi, d]$, and

$$J_g(\varphi, \psi, d)$$
$$= \begin{bmatrix} -\dfrac{fd\varphi}{(f^2+\varphi^2+\psi^2)^{\frac{3}{2}}} & -\dfrac{fd\psi}{(f^2+\varphi^2+\psi^2)^{\frac{3}{2}}} & \dfrac{f}{\sqrt{f^2+\varphi^2+\psi^2}} \\ \dfrac{d(f^2+\psi^2)}{\sqrt{f^2+\varphi^2+\psi^2}} & -\dfrac{d\varphi\psi}{(f^2+\varphi^2+\psi^2)^{\frac{3}{2}}} & \dfrac{\varphi}{\sqrt{f^2+\varphi^2+\psi^2}} \\ -\dfrac{d\varphi\psi}{(f^2+\varphi^2+\psi^2)^{\frac{3}{2}}} & \dfrac{d(f^2+\varphi^2)}{\sqrt{f^2+\varphi^2+\psi^2}} & \dfrac{\psi}{\sqrt{f^2+\varphi^2+\psi^2}} \end{bmatrix}. \qquad (28)$$

Then, we have the following estimation accuracy

$$E\left(\boldsymbol{\xi}_{k+1}\right) = 0,$$
$$D\left(\boldsymbol{\xi}_{k+1}\right) = J_g\left(\varphi, \psi, d\right) \boldsymbol{R}_{k+1} J_g^{\mathrm{T}}\left(\varphi, \psi, d\right). \quad (29)$$

From the expression of $D\left(\boldsymbol{\xi}_{k+1}\right)$, we can know that the feasible solutions to improve the calculation accuracy of current relative position from current observation are improving the observation accuracy and reducing the relative distance, et.al. As the process of rendezvous and docking goes on, the relative distance is getting smaller and smaller. So according to the (28), the accuracy of calculating the relative position will be higher and higher.

2) ESTIMATION OF THE TARGET MANEUVER
Based on the current relative position estimation obtained from the current observation, the target maneuver estimation $\hat{\boldsymbol{a}}_k$ and its estimated accuracy are given as follows.

Suppose that the state at time k is estimated as $\hat{X}_k$. Under the assumption that the noncooperative target has no maneuver, the one-step state prediction can be obtained,

$$\hat{X}_{k+1,k} = \boldsymbol{\Phi}\left(\tau\right)\hat{X}_k + \boldsymbol{G}_k\boldsymbol{u}_k. \quad (30)$$

According to (30), the one-step predicted relative position is

$$\hat{\boldsymbol{x}}_{k+1,k} = \left[\boldsymbol{\Phi}_{rr}\left(\tau\right),\ \boldsymbol{\Phi}_{rv}\left(\tau\right)\right]\hat{X}_k + \boldsymbol{\Phi}_{rv}\left(\tau\right)\boldsymbol{u}_k. \quad (31)$$

If the error of state estimation $\hat{X}_k$ is $\boldsymbol{e}_k$, i.e

$$\hat{X}_k = X_k + \boldsymbol{e}_k, \quad (32)$$

then

$$\hat{\boldsymbol{x}}_{k+1,k} = \left[\boldsymbol{\Phi}_{rr}\left(\tau\right),\ \boldsymbol{\Phi}_{rv}\left(\tau\right)\right]X_k$$
$$+ \left[\boldsymbol{\Phi}_{rr}\left(\tau\right),\ \boldsymbol{\Phi}_{rv}\left(\tau\right)\right]\boldsymbol{e}_k + \boldsymbol{\Phi}_{rv}\left(\tau\right)\boldsymbol{u}_k. \quad (33)$$

When the target has maneuver, the real state transition is

$$X_{k+1} = \boldsymbol{\Phi}\left(\tau\right)X_k + \boldsymbol{G}_k\boldsymbol{u}_k + \boldsymbol{G}_k\boldsymbol{a}_k. \quad (34)$$

So, the true relative position is

$$\boldsymbol{x}_{k+1} = \left[\boldsymbol{\Phi}_{rr}\left(\tau\right),\ \boldsymbol{\Phi}_{rv}\left(\tau\right)\right]X_k + \boldsymbol{\Phi}_{rv}\left(\tau\right)\boldsymbol{u}_k + \boldsymbol{\Phi}_{rv}\left(\tau\right)\boldsymbol{a}_k. \quad (35)$$

According to the current observation, the state is estimated to be $\tilde{\boldsymbol{x}}_{k+1}$ and the estimated error is $\boldsymbol{\xi}_{k+1}$. Then

$$\tilde{\boldsymbol{x}}_{k+1} = \left[\boldsymbol{\Phi}_{rr}\left(\tau\right),\ \boldsymbol{\Phi}_{rv}\left(\tau\right)\right]X_k$$
$$+ \boldsymbol{\Phi}_{rv}\left(\tau\right)\boldsymbol{u}_k + \boldsymbol{\Phi}_{rv}\left(\tau\right)\boldsymbol{a}_k + \boldsymbol{\xi}_{k+1}. \quad (36)$$

(37) can be obtained by (36) minus (33).

$$\boldsymbol{\Phi}_{rv}\left(\tau\right)\boldsymbol{a}_k = \tilde{\boldsymbol{x}}_{k+1} - \hat{\boldsymbol{x}}_{k+1,k}$$
$$- \left\{\boldsymbol{\xi}_{k+1} + \left[\boldsymbol{\Phi}_{rr}\left(\tau\right),\ \boldsymbol{\Phi}_{rv}\left(\tau\right)\right]\boldsymbol{e}_k\right\} \quad (37)$$

It is obvious from (7) that $\boldsymbol{\Phi}_{rv}$ is reversible. Then the target maneuver estimation, $\hat{\boldsymbol{a}}_k$, and the estimated error, $\boldsymbol{\zeta}_{k+1}$, can be obtained from (37), as shown in (38) and (39) respectively.

$$\hat{\boldsymbol{a}}_k = \boldsymbol{\Phi}_{rv}^{-1}\left(\tau\right)\left(\tilde{\boldsymbol{x}}_{k+1} - \hat{\boldsymbol{x}}_{k+1,k}\right). \quad (38)$$

$$\boldsymbol{\zeta}_{k+1} = \boldsymbol{\Phi}_{rv}^{-1}\left(\tau\right)\boldsymbol{\xi}_{k+1} + \left[\boldsymbol{\Phi}_{rv}^{-1}\left(\tau\right)\boldsymbol{\Phi}_{rr}\left(\tau\right),\ \boldsymbol{I}_3\right]\boldsymbol{e}_k. \quad (39)$$

It has been derived that $E\left(\boldsymbol{\xi}_{k+1}\right) = 0$. Further if the system state estimation at time k given by EKF is unbiased, i.e. $E\left(\boldsymbol{e}_k\right) = 0$, then $E\left(\boldsymbol{\zeta}_{k+1}\right) = 0$. That is to say, (38) gives an unbiased estimation for the target maneuver. And we can know

$$D\left(\boldsymbol{\zeta}_{k+1}\right) = \boldsymbol{\Phi}_{rv}^{-1}D\left(\boldsymbol{\xi}_{k+1}\right)\boldsymbol{\Phi}_{rv}^{-\mathrm{T}}$$
$$+ \left[\boldsymbol{\Phi}_{rv}^{-1}\left(\tau\right)\boldsymbol{\Phi}_{rr}\left(\tau\right),\ \boldsymbol{I}_3\right]\boldsymbol{P}_k\left[\boldsymbol{\Phi}_{rv}^{-1}\left(\tau\right)\boldsymbol{\Phi}_{rr}\left(\tau\right),\ \boldsymbol{I}_3\right]^{\mathrm{T}}. \quad (40)$$

Because of the maneuver estimation error of noncooperative target, the uncertainty will be introduced in the process of compensating $\hat{\boldsymbol{a}}_k$ to state equation. In this case, the error covariance matrix $\boldsymbol{Q}_k$ needs to be replaced with $\boldsymbol{Q}'_k$, where

$$\boldsymbol{Q}'_k = \boldsymbol{Q}_k + D\left(\boldsymbol{\zeta}_{k+1}.\right) \quad (41)$$

D. ALGORITHM FLOW OF DYNAMIC COMPENSATION FILTER
Next, the specific algorithm flow of DCF is given as follows:
STEP1: Calculate the alternative relative state estimation $\bar{X}_{k+1}$, the corresponding estimation error covariance matrix $\bar{\boldsymbol{P}}_{k+1}$ and the innovation $\boldsymbol{\eta}_{k+1}$ based on the state estimation, $\hat{X}_k$, and the corresponding $\boldsymbol{P}_k$ through (42) to (47)

$$\bar{X}_{k+1,k} = f\left(\hat{X}_k, \boldsymbol{u}_k\right), \quad (42)$$

$$\bar{\boldsymbol{P}}_{k+1,k} = \boldsymbol{F}_k\boldsymbol{P}_k\boldsymbol{F}_k^{\mathrm{T}} + \boldsymbol{G}_k\boldsymbol{Q}_k\boldsymbol{G}_k^{\mathrm{T}}, \quad (43)$$

$$\bar{\boldsymbol{K}}_{k+1} = \bar{\boldsymbol{P}}_{k+1,k}\boldsymbol{H}_{k+1}^{\mathrm{T}}\left(\boldsymbol{H}_{k+1}\bar{\boldsymbol{P}}_{k+1,k}\boldsymbol{H}_{k+1}^{\mathrm{T}} + \boldsymbol{R}_{k+1},\right)^{\mathrm{T}} \quad (44)$$

$$\bar{X}_{k+1} = \bar{X}_{k+1,k} + \bar{\boldsymbol{K}}_{k+1}\boldsymbol{\eta}_{k+1}, \quad (45)$$

$$\boldsymbol{\eta}_{k+1} = Z_{k+1} - h\left(\bar{X}_{k+1,k}\right), \quad (46)$$

$$\bar{\boldsymbol{P}}_{k+1} = \left(\boldsymbol{I}_6 - \bar{\boldsymbol{K}}_{k+1}\boldsymbol{H}_{k+1}\right)\bar{\boldsymbol{P}}_{k+1,k}\left(\boldsymbol{I}_6 - \bar{\boldsymbol{K}}_{k+1}\boldsymbol{H}_{k+1}\right)^{\mathrm{T}}$$
$$+ \bar{\boldsymbol{K}}_{k+1}\boldsymbol{R}_{k+1}\bar{\boldsymbol{K}}_{k+1}^{\mathrm{T}}. \quad (47)$$

STEP2: If (48) holds, set $\hat{X}_{k+1} = \bar{X}_{k+1}$, $\boldsymbol{P}_{k+1} = \bar{\boldsymbol{P}}_{k+1}$, $k = k + 1$ and go back to STEP1. Otherwise, go to STEP3.

$$\boldsymbol{\eta}_{k+1}^{\mathrm{T}}\left(\boldsymbol{H}_{k+1}\bar{\boldsymbol{P}}_{k+1,k}\boldsymbol{H}_{k+1}^{\mathrm{T}} + \boldsymbol{R}_{k+1}\right)\boldsymbol{\eta}_{k+1} < \chi_{\alpha,3}^2. \quad (48)$$

STEP3: Obtain the estimation of target maneuver, $\hat{\boldsymbol{a}}_k$, and the corresponding estimation error covariance matrix, $D\left(\boldsymbol{\zeta}_{k+1}\right)$, according to (49) to (54).

$$\tilde{\boldsymbol{x}}_{k+1}$$
$$= \left[\frac{fd}{\sqrt{f^2 + \varphi^2 + \psi^2}}, \frac{d\varphi}{\sqrt{f^2 + \varphi^2 + \psi^2}}, \frac{d\psi}{\sqrt{f^2 + \varphi^2 + \psi^2}}\right]^{\mathrm{T}}, \quad (49)$$

$J_g(\varphi, \psi, d)$

$$= \begin{bmatrix} -\dfrac{fd\varphi}{(f^2+\varphi^2+\psi^2)^{\frac{3}{2}}} & -\dfrac{fd\psi}{(f^2+\varphi^2+\psi^2)^{\frac{3}{2}}} & \dfrac{f}{\sqrt{f^2+\varphi^2+\psi^2}} \\ \dfrac{d(f^2+\psi^2)}{\sqrt{f^2+\varphi^2+\psi^2}} & -\dfrac{d\varphi\psi}{(f^2+\varphi^2+\psi^2)^{\frac{3}{2}}} & \dfrac{\varphi}{\sqrt{f^2+\varphi^2+\psi^2}} \\ -\dfrac{d\varphi\psi}{(f^2+\varphi^2+\psi^2)^{\frac{3}{2}}} & \dfrac{d(f^2+\varphi^2)}{\sqrt{f^2+\varphi^2+\psi^2}} & \dfrac{\psi}{\sqrt{f^2+\varphi^2+\psi^2}} \end{bmatrix},$$

$$(50)$$

$$\mathrm{D}(\boldsymbol{\xi}_{k+1}) = J_g(\varphi, \psi, d)\, \boldsymbol{R}_{k+1} J_g^{\mathrm{T}}(\varphi, \psi, d), \tag{51}$$

$$\hat{\boldsymbol{x}}_{k+1,k} = [\boldsymbol{\Phi}_{rr}(\tau),\ \boldsymbol{\Phi}_{rv}(\tau)]\hat{\boldsymbol{X}}_k + \boldsymbol{\Phi}_{rv}(\tau)\boldsymbol{u}_k, \tag{52}$$

$$\hat{\boldsymbol{a}}_k = \boldsymbol{\Phi}_{rv}^{-1}(\tau)\left(\tilde{\boldsymbol{x}}_{k+1} - \hat{\boldsymbol{x}}_{k+1,k}\right), \tag{53}$$

$$\mathrm{D}(\boldsymbol{\zeta}_{k+1}) = \boldsymbol{\Phi}_{rv}^{-1}\mathrm{D}(\boldsymbol{\xi}_{k+1})\boldsymbol{\Phi}_{rv}^{-\mathrm{T}} + \left[\boldsymbol{\Phi}_{rv}^{-1}(\tau)\boldsymbol{\Phi}_{rr}(\tau),\ \boldsymbol{I}_3\right]$$
$$\times \boldsymbol{P}_k\left[\boldsymbol{\Phi}_{rv}^{-1}(\tau)\boldsymbol{\Phi}_{rr}(\tau),\ \boldsymbol{I}_3\right]^{\mathrm{T}}, \tag{54}$$

STEP4: Derive the state estimation, $\hat{\boldsymbol{X}}_{k+1}$, and the corresponding $\boldsymbol{P}_{k+1}$ at time $k+1$ through (55) to (61). Set $k = k+1$ and go back to STEP1.

$$\hat{\boldsymbol{X}}_{k+1,k} = \boldsymbol{\Phi}(\tau)\hat{\boldsymbol{X}}_k + \boldsymbol{G}_k\boldsymbol{u}_k + \boldsymbol{G}_k\hat{\boldsymbol{a}}_k, \tag{55}$$

$$\boldsymbol{Q}'_k = \boldsymbol{Q}_k + \mathrm{D}(\boldsymbol{\zeta}_{k+1}), \tag{56}$$

$$\boldsymbol{P}_{k+1,k} = \boldsymbol{F}_k\boldsymbol{P}_k\boldsymbol{F}_k^{\mathrm{T}} + \boldsymbol{G}_k\boldsymbol{Q}'_k\boldsymbol{G}_k^{\mathrm{T}}, \tag{57}$$

$$\boldsymbol{K}_{k+1} = \boldsymbol{P}_{k+1,k}\boldsymbol{H}_{k+1}^{\mathrm{T}}\left(\boldsymbol{H}_{k+1}\boldsymbol{P}_{k+1,k}\boldsymbol{H}_{k+1}^{\mathrm{T}} + \boldsymbol{R}_{k+1}\right)^{\mathrm{T}}, \tag{58}$$

$$\hat{\boldsymbol{X}}_{k+1} = \hat{\boldsymbol{X}}_{k+1,k} + \boldsymbol{K}_{k+1}\boldsymbol{\eta}_{k+1}, \tag{59}$$

$$\boldsymbol{\eta}_{k+1} = \boldsymbol{Z}_{k+1} - \boldsymbol{h}\left(\hat{\boldsymbol{X}}_{k+1,k}\right), \tag{60}$$

$$\boldsymbol{P}_{k+1} = (\boldsymbol{I}_6 - \boldsymbol{K}_{k+1}\boldsymbol{H}_{k+1})\boldsymbol{P}_{k+1,k}(\boldsymbol{I}_6 - \boldsymbol{K}_{k+1}\boldsymbol{H}_{k+1})^{\mathrm{T}}$$
$$+ \boldsymbol{K}_{k+1}\boldsymbol{R}_{k+1}\boldsymbol{K}_{k+1}^{\mathrm{T}}. \tag{61}$$

IV. CONTROL SCHEME FOR RENDEZVOUS AND DOCKING

This paper does not focus on the control algorithm in the process of rendezvous and docking but adopts the multi pulse sliding guidance algorithm given in literature [22]. Here, we give the process description for the rendezvous and docking mission as well as propose the control scheme based on the relative navigation algorithm.

Assuming that the initial relative position is $\boldsymbol{x}_0$, Chaser expects to spend time T to reach the final relative position $\boldsymbol{x}_f$ through N pulses of equal time interval, $\Delta t = \frac{T}{N}$. If the chaser reaches the current position $\boldsymbol{x}_m$ with the velocity $\dot{\boldsymbol{x}}_m$ through $m-1$ times of pulses and its next destination is $\boldsymbol{x}_{m+1}$, then the pulse $\boldsymbol{u}_m$ needs to be applied at the current time m is as follows

$$\boldsymbol{u}_m = \boldsymbol{\Phi}_{rv}^{-1}(\Delta t)(\boldsymbol{x}_{m+1} - \boldsymbol{\Phi}_{rr}(\Delta t)\boldsymbol{x}_m) - \dot{\boldsymbol{x}}_m. \tag{62}$$

In this paper, the initial relative state is assumed to be $\boldsymbol{X}_0 = [-100, -100, -100, 0, 0, 0]^{\mathrm{T}}$, where the unit of the relative position is meter (m) and the unit of the relative velocity is meter $\cdot$ second^{-1} (m $\cdot$ s^{-1}). The initial state estimation $\hat{\boldsymbol{X}}_0 = [-90, -120, -90, 0, 0, 0]^{\mathrm{T}}$. It is expected that the final relative position will be reached through 50 pulses and the total time cost $T = 500$ s. All target positions are
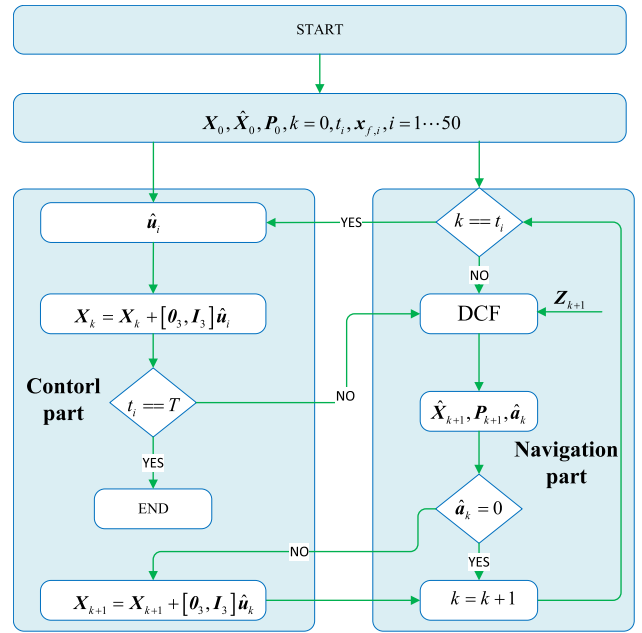

FIGURE 3. Schematic diagram of docking with noncooperative targets.

V. SIMULATIONS

recorded as $\boldsymbol{x}_{f,i} = \boldsymbol{x}_0 + \frac{i}{50}(\boldsymbol{x}_f - \boldsymbol{x}_0)$, $i = 1, \cdots 50$. Then the required pulses are $\boldsymbol{u}_i$, $i = 1 \cdots 50$. Their value can be calculated by (62) and the corresponding pulse application time $t_i = (i-1)\Delta t$, $i = 1, \cdots 50$.

Remark5: It should be pointed out that the relative state needs to be estimated. So the true maneuver $\hat{\boldsymbol{u}}$ given by the system may be different from the ideal maneuver, $\boldsymbol{u}$, which may lead to the deviation between the actual control trajectory and the ideal control trajectory. However, once the self-pulse is given, it is regarded as the known input and does not affect the estimation performance of filters.

Remark6: When the noncooperative target has unknown maneuver, the rendezvous and docking task cannot be completed only depending on the above guidance algorithm. The scheme given in this paper is as follows. When the target maneuver is detected, the chaser recalculates the required pulse according to (62) to counteract the impact of the target maneuver and ensures that the chaser reach the predetermined relative state at the predetermined time. However, it should be noted that when the observation interval is τ, there is also a time delay for the estimation of target maneuver. So, it also takes a time delay for the chaser to offset the effect of target maneuver through its own maneuver.

To sum up, the navigation and control scheme of rendezvous and docking with the maneuvering noncooperative target are shown in Fig. 3.

V. SIMULATIONS

In this section, the navigation and control scheme are verified through numerical simulations. Firstly, in addition to those have been given in Section 3, other simulation parameters are listed in Table. 1.

TABLE 1. Simulation parameters.

Q_k	σ_φ(mm)	σ_ψ(mm)	σ_d(mm)	f(mm)	τ(s)	P_0	α	ω(rad/s)
I_3	0.1	0.1	1	35	1	I_6	0.99	0.001

TABLE 2. Estimation results and final control errors comparision under no target maneuver.

	poisition estimation RMSE (cm)			velocity estimation RMSE (cm/s)			final control errors (cm)
	x	y	z	x	y	z	
EKF	0.4749	1.4172	1.3969	0.8230	2.3592	2.2725	0.58
DCF	0.5837	1.2876	1.4265	1.0456	1.9068	2.1327	0.98

(a) Real trajectory and estimated trajectory

(b) Final control error
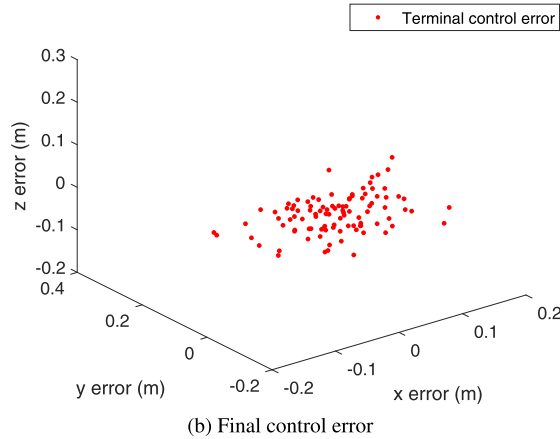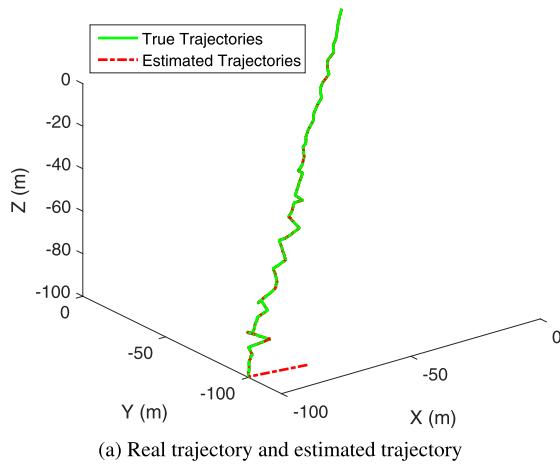
FIGURE 4. Estimation results by DCF under no target maneuver.

Consider the following three kinds of maneuvers for the noncooperative target:
(1) The noncooperative target has no maneuver i.e. $a_k = 0 \text{ m} \cdot \text{s}^{-2}$.
(2) The noncooperative target has constant unknown maneuver and $a_k = \begin{cases} [-10, -10, 10] \text{ m} \cdot \text{s}^{-2} & 150 \le k \le 350 \\ [0, 0, 0] \text{ m} \cdot \text{s}^{-2} & \text{else} \end{cases}$
(3) The noncooperative target has time-varying unknown maneuver and $a_k = \begin{cases} [10, -50, -50] \cdot \sin(0.3k) \text{ m} \cdot \text{s}^{-2} & 150 \le k \le 350 \\ [0, 0, 0] \text{ m} \cdot \text{s}^{-2} & \text{else} \end{cases}$
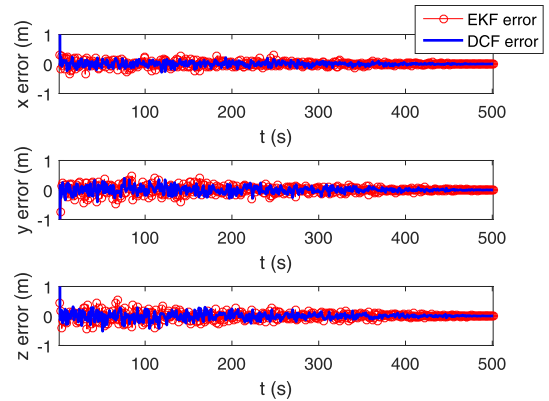
(a) Relative position estimation error
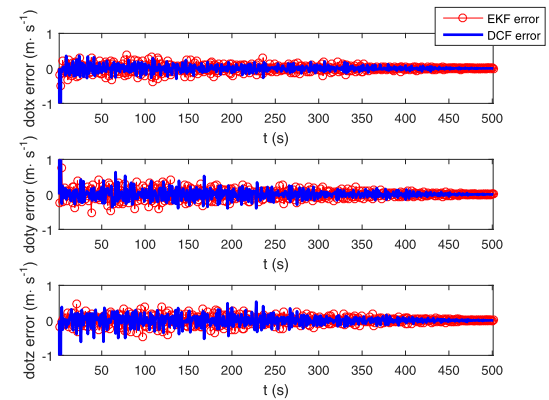
(b) Relative velocity estimation error

FIGURE 5. State estimation result comparsion under no target maneuver.

According to the above three kinds of target maneuvers, 100 Monte Carlo simulation experiments are carried out respectively and the simulation results are given in the next three subsections.

It should be noted that for different target maneuvers, the computational performance of different estimators and corresponding control schemes are evaluated through the following two aspects. First, the control performance is assessed by the final control errors, i.e. the differences between the final position reached by different control schemes and the planned one. The second is the performance of relative state estimation. When the target makes different maneuvers, the control schemes based on different estimators will lead to different real relative states. For example, if the control scheme based on EKF results in x_k^{EKF} and the state estimation obtained by EKF is $\hat{x}_k^{\text{EKF}}$, then its estimation error $\text{Error}^{\text{EKF}} = x_k^{\text{EKF}} - \hat{x}_k^{\text{EKF}}$. Similarly, the relative state estimation error of DCF $\text{Error}^{\text{DCF}} = x_k^{\text{DCF}} - \hat{x}_k^{\text{DCF}}$, where x_k^{DCF} and $\hat{x}_k^{\text{DCF}}$ are the true relative state given by DCF-based control scheme and state estimation obtained by DCF. The smaller the estimation error means the higher the relative state estimation accuracy.

A. SIMULATIONS WITHOUT TARGET MANEUVER
In the case of no target maneuver, the real trajectory in a certain experiment and the estimated trajectory obtained by the
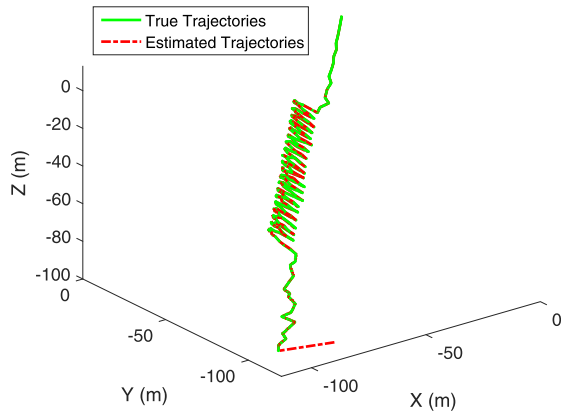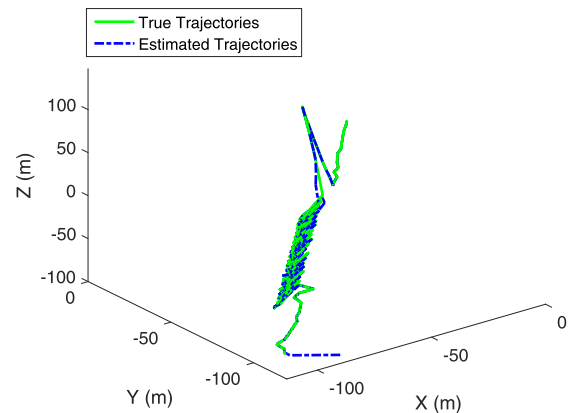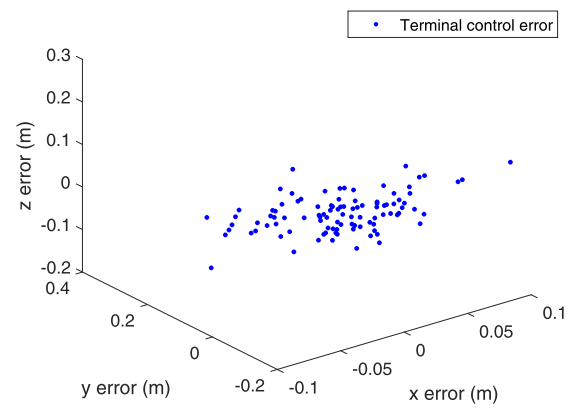
(a) Real trajectory and estimated trajectory
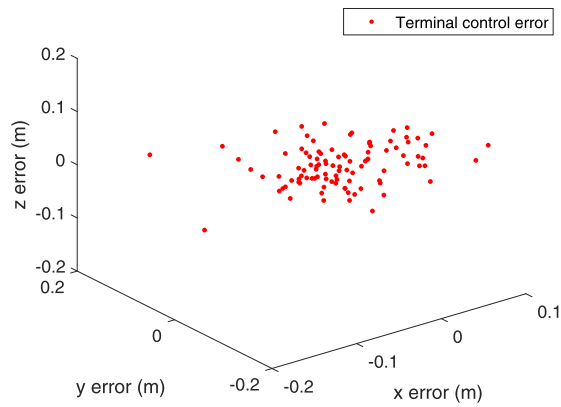
(b) Final control error

FIGURE 6. Estimation results by DCF under constant target maneuver.

(a) Real trajectory and estimated trajectory

(b) Final control error

FIGURE 7. Estimation results by VSDE under constant target maneuver.

proposed algorithm are shown in Fig. 4 (a). Fig. 4 (b) shows the final control errors of 100 times of Monte Carlo simulations. Fig. 5 shows the position and velocity estimation errors of DCF and EKF. It is worth noting that the true control trajectory obtained by EKF may be different that given by DCF. The estimated errors here are the difference between the respectively real trajectory and the estimated one. Table. 2 shows the root mean square error (RMSE) of the relative state estimation on three directions, x, y, z, and the average final control errors obtained by EKF and DCF through 100 Monte Carlo simulations. Here, the estimation errors refer to those after the time $k = 5$, i.e. after the two filters converge.

From Fig. 4 (b), it can be seen that the three components of the final control errors are basically less than 0.2 m. Fig. 4 (a) and Fig. 5 illustrate that DCF is broadly consistent with EKF. As Table. 2 shows, the RMSE and the final control errors given by EKF and DCF are equivalent, which means that the proposed estimator is at least better than EKF.

B. SIMULATIONS WITH CONSTANT TARGET MANEUVER
In this paper, variable state dimension estimator (VSDE) [17] [28] is applied to make a comparative test for the case that the target has unknown maneuvers. When the

noncooperative target maneuver is detected, the state vector is augmented to X_k^{aug},

$$X_k^{\text{aug}} = \left[X_k^{\text{T}} \ a_k^{\text{T}}\right]^{\text{T}}. \tag{63}$$

If the acceleration of the noncooperative target is assumed to be constant, the corresponding state transfer equation is as follows,

$$\begin{bmatrix} X_{k+1} \\ a_{k+1} \end{bmatrix} = \begin{bmatrix} \Phi(\tau) \ G_k \\ 0_{3\times6} \ I_3 \end{bmatrix} \begin{bmatrix} X_k \\ a_k \end{bmatrix} + \begin{bmatrix} G_k u_k \\ 0_{3\times1} \end{bmatrix}. \tag{64}$$

According to the new state transition equation, VSDE can construct the corresponding filter which is omitted here. Remarkably, when the noncooperative target maneuver is detected, the initial target acceleration estimation should be given and the estimation error covariance matrix need to be reset by (65).

$$P_k^{\text{aug}} = \begin{bmatrix} P_k \ 0_{6\times3} \\ 0_{3\times6} \ P_k^{\text{a}} \end{bmatrix}. \tag{65}$$

Here, the initial target maneuver estimation is set to $\left[-5 \ -5 \ 5\right]^{\text{T}}$ and the corresponding estimation error covariance matrix is set to be I_3.

Fig. 6 (a), Fig. 7 (a) and Fig. 8 (a) respectively show the real trajectory and the estimated one given by the DCF, VSDE
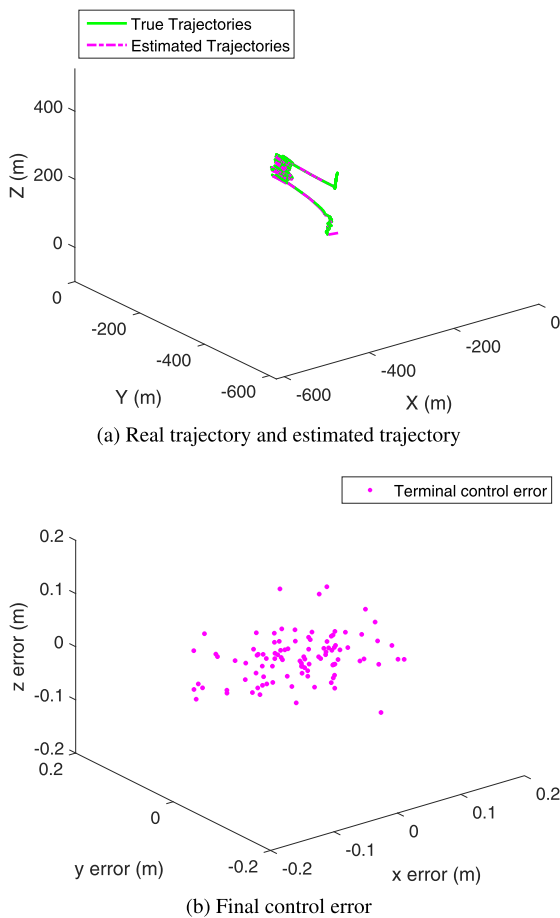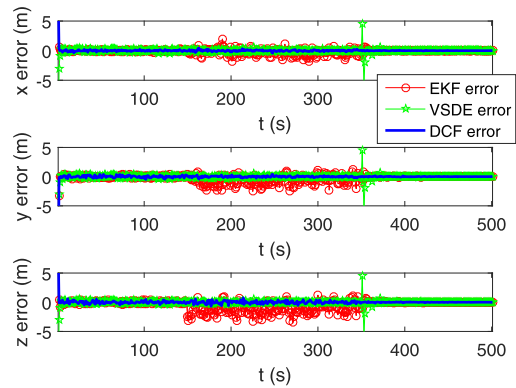
(a) Real trajectory and estimated trajectory

(b) Final control error

FIGURE 8. Estimation results by EKF under constant target maneuver.

(a) Relative position estimation error

(b) Relative velocity estimation error

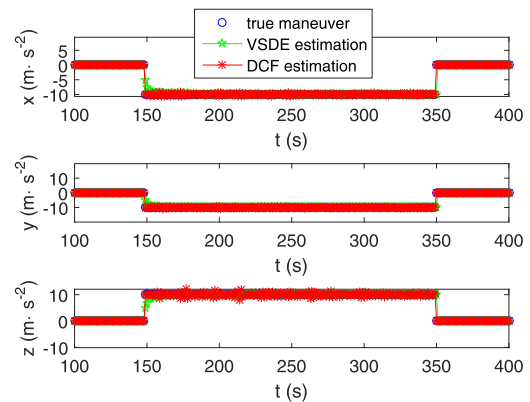**FIGURE 9.** State estimation result comparsion under constant target maneuver.

FIGURE 10. Target maneuver estimation and real constant target maneuver.

and EKF based navigation control schemes when the target has constant unknown maneuver. Fig. 6 (b), Fig. 7 (b) and Fig. 8 (b) give the final control errors obtained by 100 times of Monte Carlo simulations under three control schemes. Fig. 9 draws the relative position and velocity estimation errors obtained by three estimators. Fig. 10 presents the real constant target maneuver and the estimated ones obtained by DCF and VSDE. Table. 3 shows the relative state estimation RMSE from time 5 to 350 of the three estimators and the final control errors when the target has the unknown constant maneuver.

As can be seen from Fig. 9, when the noncooperative target is in constant maneuvering, the EKF performance decreases. By contrast, VSDE and DCF can maintain higher relative state estimation accuracy. However, at the end of target maneuver, due to the reset of estimation error covariance matrix, VSDE experienced a short period of turbulence. On the contrary, the proposed estimator can pass the maneuver transition period smoothly.

Due to the difference of relative state estimation, the real control trajectories in the subgraphs (a) of Fig. 6 to Fig. 8 differ. However, since the three estimators all converge again after the end of target maneuver, the final control errors of the three control schemes are small and have

no significant difference, as shown in the subgraphs (b) of Fig. 6 to Fig. 8.

According to Fig. 10, both VSDE and DCF can estimate the constant target maneuver with high accuracy. However, because VSDE cannot provide accurate initial maneuver estimation, it needs a short time to converge after the start of target maneuver.

From Table 3, due to the correct model assumption, the relative state estimation accuracy of VSDE is equivalent to that of DCF, and both are higher than that of EKF. However,

TABLE 3. Estimation results and final control errors comparision under constant target maneuver.

	position estimation RMSE (cm)			velocity estimation RMSE (cm/s)			final control errors (cm)
	x	y	z	x	y	z	
EKF	23.53	51.77	106.56	16.12	29.87	85.98	1.26
VSDE	1.2983	2.3763	4.7256	2.1419	3.8430	7.3880	1.96
DCF	1.4720	2.2313	3.8523	2.5907	3.5303	7.4324	1.25

(a) Real trajectory and estimated trajectory
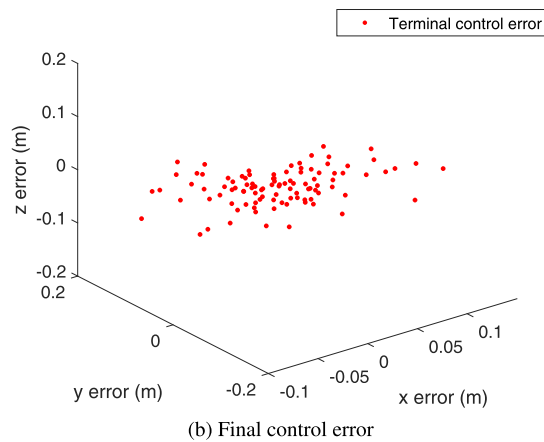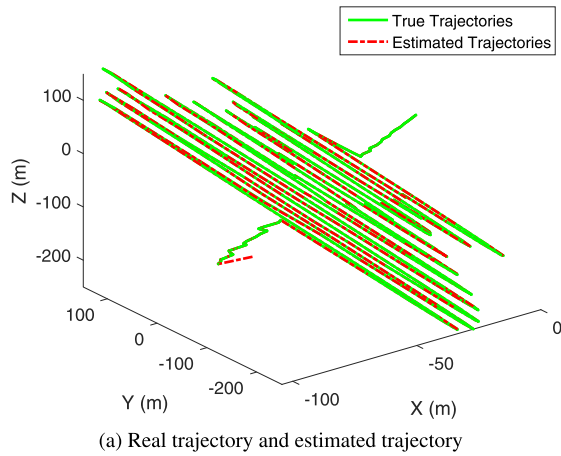

(b) Final control error

FIGURE 11. Estimation results by DCF under time-varying target maneuver.

it should be noted that, as shown in Figure 10, after time 350, VSDE experiences a short period of turbulence due to the reset of the estimation error covariance matrix, which may reduce the accuracy of its relative state estimation.

C. SIMULATIONS WITH TIME-VARYING TARGET MANEUVER

For the navigation and control in the case of time-varying target maneuver, this paper also makes comparative simulation experiments with DCF, VSDE and EKF. Fig. 11 (a) shows the real and the corresponding estimated trajectory given by DCF. Fig. 11 (b) presents the final control errors of the DCF-based scheme. Fig. 12 draws the estimation errors of three kinds of estimators under the condition of time-varying maneuvering.
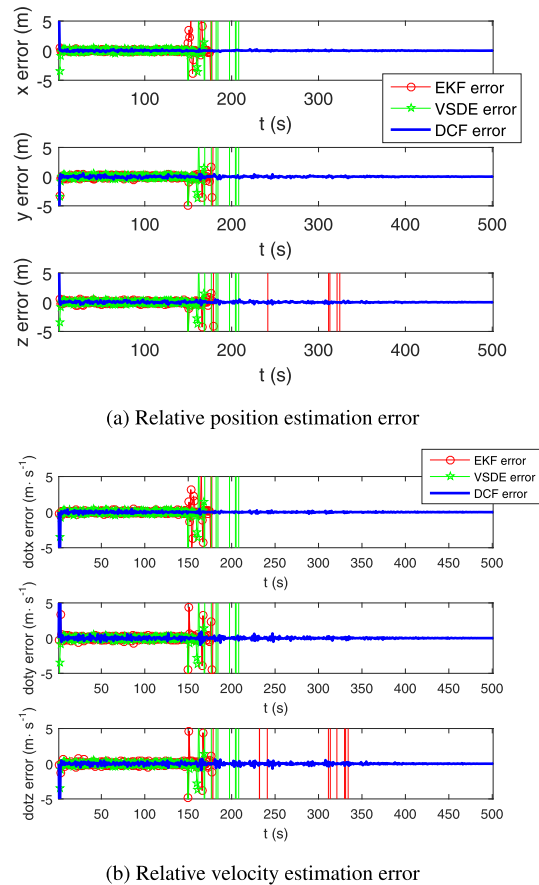

(a) Relative position estimation error

(b) Relative velocity estimation error

FIGURE 12. State estimation result comparsion under time-varying target maneuver.
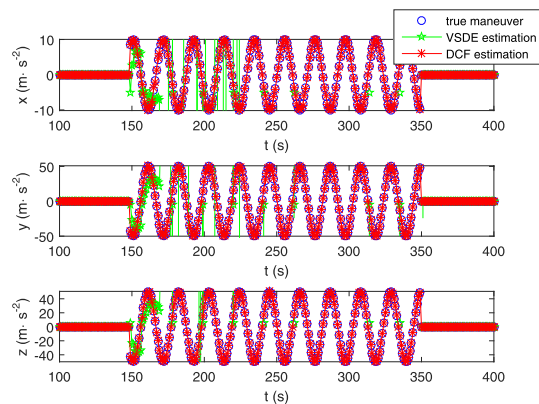

FIGURE 13. Maneuver estimation and real time-varying target maneuver.

Fig. 13 shows the real target maneuver and the estimated obtained by DCF and VSDE.

It can be seen from Fig. 13 that when the noncooperative target has time-varying maneuver, the maneuvering estimation deviation of VSDE becomes larger and larger. As is shown in Fig. 12, EKF and VSDE diverge rapidly with the emergence of time-varying maneuver, which leads to great control errors and failure of the rendezvous mission. In contrast, Fig. 11 to Fig. 13 show that DCF performs satisfactorily in the estimation of the target maneuver and the relative state.

The control scheme based on DCF still can complete the rendezvous and docking task commendably.

Remark7: The simulation results demonstrate that the performance of DCF is consistent with that of EKF in the case of no target maneuver. When the noncooperative target have unknown constant maneuver, the proposed algorithm is more stable than EKF and VSDE. Both EKF and VSED fail to estimate the time-varying target maneuver as well as diverge when the time-varying maneuver occurs. The space rendezvous and docking task cannot be completed by the control scheme based on VSDE and EKF. On the contrary, DCF performs excellently although the target maneuver varies with time.

VI. CONCLUSION

This paper discusses the navigation and control scheme used for space rendezvous and docking with maneuvering non-cooperative targets. A relative measurement scheme based on only one monocular camera and one distance sensor is designed firstly. Afterwards, DCF is proposed to estimate the relative state and target maneuver. Based on DCF, the control scheme is derived for the space rendezvous and docking task with the maneuvering target. The simulation results prove that the performance of the proposed estimator is equivalent to EKF in the case of no target maneuver. DCF outperforms EKF and VSDE when the noncooperative target has constant maneuver. When the target maneuvering changes with time, the navigation and control scheme based on DCF can complete the space rendezvous and docking task, while the task cannot be accomplished by other two control schemes.
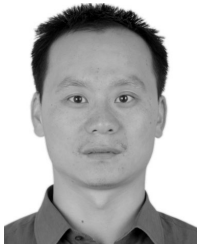
REFERENCES

[1] M. A. Baird, "Maintaining space situational awareness and taking it to the next level," *Air Space Power J.*, vol. 27, no. 5, pp. 50–72, Sep/Oct. 2013.

[2] L. Zhang, D.-M. Wu, and Y. Ren, "Pose measurement for non-cooperative target based on visual information," *IEEE Access*, vol. 7, pp. 106179–106194, 2019.

[3] G. Gaias, S. D'Amico, and J.-S. Ardaens, "Angles-only navigation to a noncooperative satellite using relative orbital elements," *J. Guid., Control, Dyn.*, vol. 37, no. 2, pp. 439–451, Mar. 2014.

[4] L. Sun, W. Huo, and Z. Jiao, "Adaptive backstepping control of spacecraft rendezvous and proximity operations with input saturation and full-state constraint," *IEEE Trans. Ind. Electron.*, vol. 64, no. 1, pp. 480–492, Jan. 2017.

[5] Y. Liu, Y. Lyu, and G. Ma, "6-DOF multi-constrained adaptive tracking control for noncooperative space target," *IEEE Access*, vol. 7, pp. 48739–48752, 2019.

[6] H. Wang, B. Yang, Y. Liu, W. Chen, X. Liang, and R. Pfeifer, "Visual servoing of soft robot manipulator in constrained environments with an adaptive controller," *IEEE/ASME Trans. Mechatronics*, vol. 22, no. 1, pp. 41–50, Feb. 2017.

[7] Y. Liu, R. Xiong, Y. Wang, H. Huang, X. Xie, X. Liu, and G. Zhang, "Stereo visual-inertial odometry with multiple Kalman filters ensemble," *IEEE Trans. Ind. Electron.*, vol. 63, no. 10, pp. 6205–6216, Oct. 2016.

[8] J. Luo, B. Gong, J. Yuan, and Z. Zhang, "Angles-only relative navigation and closed-loop guidance for spacecraft proximity operations," *Acta Astronautica*, vol. 128, pp. 91–106, Nov. 2016.

[9] Y. Zhang, P. Huang, K. Song, and Z. Meng, "An angles-only navigation and control scheme for noncooperative rendezvous operations," *IEEE Trans. Ind. Electron.*, vol. 66, no. 11, pp. 8618–8627, Nov. 2019.

[10] R. D. Coder and M. J. Holzinger, "Multi-objective design of optical systems for space situational awareness," *Acta Astronautica*, vol. 128, pp. 669–684, Nov. 2016.

[11] Z. Guang, B. Xingzi, Z. Hanyu, and L. Bin, "Non-cooperative maneuvering spacecraft tracking via a variable structure estimator," *Aerosp. Sci. Technol.*, vol. 79, pp. 352–363, Aug. 2018.

[12] R. Liu, Z. Sun, and D. Ye, "Adaptive sliding mode control for spacecraft autonomous rendezvous with elliptical orbits and thruster faults," *IEEE Access*, vol. 5, pp. 24853–24862, 2017.

[13] B. Jia and M. Xin, "Vision-based spacecraft relative navigation using sparse-grid quadrature filter," *IEEE Trans. Control Syst. Technol.*, vol. 21, no. 5, pp. 1595–1606, Sep. 2013.

[14] J. Grzymisch and W. Fichter, "Observability criteria and unobservable maneuvers for in-orbit bearings-only navigation," *J. Guid., Control, Dyn.*, vol. 37, no. 4, pp. 1250–1259, Jul. 2014.

[15] J. Grzymisch and W. Fichter, "Analytic optimal observability maneuvers for in-orbit bearings-only rendezvous," *J. Guid., Control, Dyn.*, vol. 37, no. 5, pp. 1658–1664, Sep. 2014.

[16] R. Volpe and C. Circi, "Optical-aided, autonomous and optimal space rendezvous with a non-cooperative target," *Acta Astronautica*, vol. 157, pp. 528–540, Apr. 2019.

[17] S. Lee, J. Lee, and I. Hwang, "Maneuvering spacecraft tracking via state-dependent adaptive estimation," *J. Guid., Control, Dyn.*, vol. 39, no. 9, pp. 2034–2043, Sep. 2016.

[18] S. Hu, J. Zhou, and C. Chen, "State estimation for dynamic systems with unknown process inputs and applications," *IEEE Access*, vol. 6, pp. 14857–14869, 2018.

[19] G. M. Goff, J. T. Black, and J. A. Beck, "Orbit estimation of a continuously thrusting satellite using variable dimension filters," in *Proc. AIAA Guid., Navigat., Control Conf.*, Kissimmee, Florida, USA, Jan. 2015.

[20] E. Bekir, "Adaptive Kalman filter for tracking maneuvering targets," *J. Guid., Control, Dyn.*, vol. 6, no. 5, pp. 414–416, Sep. 1983.

[21] J. Wang, T. Zhang, X. Xu, and Y. Li, "A variational Bayesian based strong tracking interpolatory cubature Kalman filter for maneuvering target tracking," *IEEE Access*, vol. 6, pp. 52544–52560, 2018.

[22] R. Singer, "Estimating optimal tracking filter performance for manned maneuvering targets," *IEEE Trans. Aerosp. Electron. Syst.*, vols. AES-6, no. 4, pp. 473–483, Jul. 1970.

[23] Y. Chan, A. Hu, and J. Plant, "A Kalman filter based tracking scheme with input estimation," *IEEE Trans. Aerosp. Electron. Syst.*, vols. AES-15, no. 2, pp. 237–244, Mar. 1979.

[24] S. Li, X. Jiang, and Y. Liu, "Innovative Mars entry integrated navigation using modified multiple model adaptive estimation," *Aerosp. Sci. Technol.*, vol. 39, pp. 403–413, Dec. 2014.

[25] X. Li and Y. Bar-Shalom, "Design of an interacting multiple model algorithm for air traffic control tracking," *IEEE Trans. Control Syst. Technol.*, vol. 1, no. 3, pp. 186–194, Sep. 1993.

[26] B. Han, H. Huang, L. Lei, C. Huang, and Z. Zhang, "An improved IMM algorithm based on STSRCKF for maneuvering target tracking," *IEEE Access*, vol. 7, pp. 57795–57804, 2019.

[27] W. Youn and H. Myung, "Robust interacting multiple model with modeling uncertainties for maneuvering target tracking," *IEEE Access*, vol. 7, pp. 65427–65443, 2019.

[28] Z. Guang, Z. Hanyu, W. Qiuqiu, and L. Bin, "Relative motion and thrust estimation of a non-cooperative maneuvering target with adaptive filter," *Acta Astronautica*, vol. 162, pp. 98–108, Sep. 2019.

[29] M. Okasha and B. Newman, "Guidance, navigation and control for satellite proximity operations using Tschauner-Hempel equations," *J. Astron. Sci.*, vol. 60, no. 1, pp. 109–136, Mar. 2013.

[30] D. C. Woffinden and D. K. Geller, "Optimal orbital rendezvous maneuvering for angles-only navigation," *J. Guid., Control, Dyn.*, vol. 32, no. 4, pp. 1382–1387, Jul. 2009.

[31] E. W. Frew and S. M. Rock, "Trajectory generation for constant velocity target motion estimation using monocular vision," in *Proc. IEEE Int. Conf. Robot. Automat.*, Taipei, China, Mar. 2003, pp. 3479–3484.

[32] J. Yi, H. Wang, J. Zhang, D. Song, S. Jayasuriya, and J. Liu, "Kinematic modeling and analysis of skid-steered mobile robots with applications to low-cost inertial-measurement-unit-based motion estimation," *IEEE Trans. Robot.*, vol. 25, no. 5, pp. 1087–1097, Oct. 2009.

[33] H. Lee and M.-J. Tahk, "Generalized input-estimation technique for tracking maneuvering targets," *IEEE Trans. Aerosp. Electron. Syst.*, vol. 35, no. 4, pp. 1388–1402, Oct. 1999.

DONGHUI LYU received the B.S. degree in information and computing sciences from the University of Science and Technology Beijing, Beijing, China, in 2014. He is currently pursuing the master's degree with the National University of Defense Technology. His current research interests include Kalman filter, signal processing, and integrated navigation.

JIONGQI WANG received the B.S. degree in applied mathematics from Zhejiang University, Hangzhou, China, in 2002, and the M.S. and Ph.D. degrees in system science from the National University of Defense Technology, Changsha, China, in 2004 and 2008, respectively. From 2008 to 2013, he was a Lecturer with the National University of Defense Technology, where he has been an Associate Professor with the College of Liberal Arts and Sciences, since 2014. His interests in big data analysis, parameter estimation, system identification, and satellite state filter and its applications. He conducts several outstanding research awards from the National Natural Science Foundation of China and Ministry of Education of China.

ZHANGMING HE received the B.S. and M.S. degrees in applied mathematics and the Ph.D. degree in system science from the National University of Defense Technology, Changsha, China, in 2008, 2010, and 2015, respectively. From 2013 to 2014, he was a Visiting Scholar with the Institute for Automatic Control and Complex Systems, University of Duisburg-Essen, Duisburg, Germany. Since 2015, he has been a Lecturer with the College of Liberal Arts and Sciences, National University of Defense Technology, Changsha. He has published more than ten refereed journal articles and 15 international conference papers, coauthored two monographs, and holds six patents. His interests in fault diagnosis and prognosis, signal processing, and system identification.

BOWEN HOU received the B.S. and M.S. degrees in applied mathematics from the National University of Defense Technology, in 2012 and 2016, respectively, where he is currently pursuing the Ph.D. degree. His research interests include navigation, filter, data processing, and data fusion.

HAIYIN ZHOU received the B.S. degree in applied mathematics from Wuhan University, Wuhan, China, in 1986, the M.S. degree from Hunan University, Changsha, China, in 1989, and the Ph.D. degree in systems engineering from the National University of Defense Technology, Changsha, in 2003.

Since 2009, he has been a Professor with the College of Liberal Arts and Sciences, National University of Defense Technology. He currently serves as a part-time Researcher with the Beijing Institute of Control Engineering, Beijing, China. He has published more than 80 refereed journal articles and ten international conference papers, coauthored four monographs, and six patents. His interests in data driven diagnosis approaches, power system dynamics and controls, advanced signal processing, and data information fusion and its application.

DAYI WANG received the Ph.D. degree in aerospace engineering from the Harbin Institute of Technology, in 2003.

From 2003 to 2015, he was a Researcher with the Beijing Institute of Spacecraft System Engineering, China Academy of Space Technology. From 2011 to 2015, he was the Deputy Director of the State Key Laboratory of Spatial Intelligent Control Technology and was the Chief Scientist for the 973-Project. He was authorized with 34 patents, published two monographs, and more than 69 articles.

Dr. Wang received the National Outstanding Youth Fund of National Natural Science Foundation of China. He conducted innovative research in the field of spacecraft autonomous navigation and control and solved a series of key technical issues.

• • •